

Application of the Ensemble Kalman Filter and Smoother to a Coupled Atmosphere-ocean Model

Genta Ueno¹, Tomoyuki Higuchi¹, Takashi Kagimoto², and Naoki Hirose³

¹*The Institute of Statistical Mathematics, ROIS/Japan Science and Technology Agency, Tokyo, Japan*

²*Frontier Research Center for Global Change/JAMSTEC, Yokohama, Japan*

³*Research Institute for Applied Mechanics, Kyushu University, Fukuoka, Japan*

Abstract

We report an application of the ensemble Kalman filter (EnKF) and smoother (EnKS) to an intermediate coupled atmosphere-ocean model of Zebiak and Cane, into which the sea surface height (SSH) anomaly observations by TOPEX/POSEIDON (T/P) altimetry are assimilated. Smoothed estimates of the 54,403 dimensional state are obtained from 1,981 observational points with 2,048 ensemble members. While assimilated data are SSH anomalies alone, the estimated sea surface temperature (SST) anomalies reproduce primary temporal characteristics of the actual SST. The smoothed estimate of the zonal wind anomalies is also consistent with the observation except for the westerly anomalies in the western Pacific.

1. Introduction

The El Niño-Southern Oscillation (ENSO) phenomenon is a dominant climate variation on interannual timescales, and it depends essentially upon coupled interactions of the dynamics of ocean and atmosphere (Neelin et al. 1998). ENSO is characterized by quasiperiodic interannual oscillation of tropical Pacific sea surface temperatures (SSTs) with a dominant period of approximately 4 years. Since ENSO affects not only global climate but ecosystems in and around the tropical Pacific and economies of several countries, successful prediction of ENSO is of great interest from scientific and social points of view (Latif et al. 1998).

With a coupled atmosphere-ocean model, Zebiak and Cane (1987) (hereinafter referred to as ZC) have provided the first successful ENSO prediction. The ZC model is a nonlinear anomaly model of intermediate complexity and reproduces an ENSO-like quasiperiodic variation. On the basis of intermediate coupled models, data assimilation studies have been carried out for better prediction and reanalysis of ENSO events. Assimilation methods adopted to the coupled models range from simple schemes of nudging (Chen et al. 1995, 1998) or direct insertion (Chen et al. 1999) to advanced ones such as the representer method (Bennett et al. 1998, 2000), the adjoint method (Lee et al. 2000), a reduced-order Kalman filter (ROKF, Ballabrera-Poy et al. 2001), or the extended Kalman filter (EKF, Sun et al. 2002).

Advanced schemes are characterized by their clear assumptions based on the dynamical and statistical implications, which are in contrast to ad hoc assumptions of simple schemes (e.g., Fukumori 2001). However, the advanced schemes listed above could not treat the ZC coupled model without modification or approximation. When the above two variational methods (the representer method and the adjoint method) were applied, the atmospheric component was modified or simplified in order to derive the adjoint equations. The two sequential methods (ROKF and EKF) require a linear approximation of the nonlinear model. It means that the advanced schemes may

degrade the model's ability to reproduce nonlinear physical processes.

In addition, neglected system noise or Gaussian system noise employed by these works is another problem. If the model dynamics is assumed to be perfect (so-called "the strong constraint"), and the optimal initial and/or boundary conditions are estimated, assimilation experiments are carried out under the system noise-free condition (Lee et al. 2000; Ballabrera-Poy et al. 2001). Apparently the assumption of perfect models is questionable for simple coupled models as the ZC model. On the other hand, the weak constraint was employed by Bennett et al. (1998) and Sun et al. (2002); they assumed Gaussian system noise added to the model equation. This system model is reasonable compared with the strong constraint. The weak constraint model is, however, still questionable because the Gaussian system noise is added to all of state variables. Since the model includes nonlinear transformation, Gaussian perturbation is converted to non-Gaussian perturbation, and some of the system variables then should be affected by non-Gaussian system noise. However, it is difficult to set alternative noise suitable for nonlinear systems and this is actually impossible for the ROKF and the EKF because system noise is treated with covariance matrices.

The ensemble Kalman filter (EnKF, Evensen 2003; Miyoshi 2005) can solve these problems. First, the EnKF can handle dynamic models without any modification or approximation since the EnKF requires neither linearized model nor adjoint model. Second, the EnKF can easily introduce a non-Gaussian system noise appropriate to nonlinear models. The EnKF treats the system noise by realizations generated from an assumed distribution. When we impose the realizations of the system noise on certain variables, their effects are conveyed to other variables according to the model equation. As a result, even if the imposed realizations are from Gaussian, effects received by the other variables may be non-Gaussian which can be considered as the system noise consistent with the nonlinear model. These two advantages of the EnKF would produce more accurate prediction error (Ueno et al. 2006a). In addition, the EnKF can provide reasonable initial perturbations for ensemble forecasting.

In spite of these advantages, the EnKF has not been applied to coupled atmosphere-ocean models as far as the authors examined. One reason may be a required computational load of the EnKF (Ueno et al. 2006b). In the present paper we report the first application of the EnKF to a coupled atmosphere-ocean model. In Section 2, the ZC model is outlined, into which the sea surface height (SSH) anomaly observations by TOPEX/POSEIDON (T/P) altimetry are assimilated. An EnKF experiment is then shown, followed by an experiment of the ensemble Kalman smoother (EnKS, Evensen 2003), a smoothing algorithm designed for ensemble-based approaches. Since smoothed states reflect future observations as well as past observations, the estimates adjust the time delay found in the filtered estimates and allow us to examine time dependent causality. We examine the estimated temporal variations of the SST and trade wind indices. Summary and discussion are given in Section 3.

Corresponding author: Genta Ueno, The Institute of Statistical Mathematics, ROIS, 4-6-7 Minami-Azabu, Minato-ku, Tokyo 106-8569, Japan. E-mail: gen@ism.ac.jp. ©2007, the Meteorological Society of Japan.

2. EnKF and EnKS experiments

2.1 Simulation model and data

The ZC model couples two linear shallow-water equations: a steady-state atmospheric model and a dynamic reduced-gravity ocean model. The atmospheric component is forced by heating that depends on SST and surface wind convergence. The SST evolves in time according to the thermodynamic equation. The ocean component is forced by surface wind stress calculated from surface wind through the bulk formula. The ZC model includes nonlinear equations for the heating due to the surface wind convergence and for the wind stress. All variables are anomalies with respect to the prescribed monthly mean climatology, and they consist of the horizontal ocean current \mathbf{u} in the upper layer, the thermocline depth h , the SST T , the atmospheric wind \mathbf{u}_a , the surface wind convergence c , heating due to SST Q_s , and the wind stress $\boldsymbol{\tau}$. The ocean model is regional and extends from 124°E to 80°W and from 29°N to 29°S, in which \mathbf{u} and h are defined at grid points of $2^\circ \times 0.5^\circ$ resolution, while T and $\boldsymbol{\tau}$ are computed at coarser grid points of $5.625^\circ \times 2^\circ$ interval. The atmospheric model, on the other hand, is global, and \mathbf{u}_a is defined at $5.625^\circ \times 2^\circ$ grid points. The dimension of the state vector of the ZC model is 54,403.

We assimilate the T/P SSH anomaly observations by the Altimeter Ocean Pathfinder from its repeat cycle 1 to 364 (from September 23, 1992 to August 11, 2002; each cycle takes 9.915625 days). While the data are provided at $1^\circ \times 1^\circ$ spatial resolution, we use those at the grid points every $L_x = 4^\circ$ in the zonal and $L_y = 2^\circ$ in the meridional directions inside the model ocean basin. We avoid using data outside of the Pacific (that is, those in Arafura Sea, Gulf of Mexico, and Caribbean Sea). The number of data points at each cycle is usually 1,981, but it may decrease down to 1,720 due to partially missing data, and at cycle 118 the data are totally missing.

The ZC model does not solve the SSH anomaly itself. It does, instead, compute the thermocline depth anomaly h , which can be converted into the SSH through the isostatic relation as $(g'/g)h$ where g (g') is the (reduced) gravity and $g'/g = 0.00573$.

Figures 1a and 1b show SSH anomalies along the equator observed by T/P, and those reproduced by the ZC model without data assimilation, respectively. Model time step is set to be identical to the T/P sampling interval, 9.915625 days, and spin-up period is set to 90 years, when the characteristic standing oscillation is reproduced (ZC). The model output displays a periodic oscillation that includes large El Niño events in 1993/94 and 1997/98, and La Niña in 1995/96 and 1999/2000. Concurrences of some peaks are coincidences; even slightly different spin-up periods may shift these peaks forward or backward in time. Apparently the reproduced variations have many aspects inconsistent with the T/P observation. For example, neither the 1993/94 El Niño event is the case, nor positive anomalies observed in the western Pacific are identified in the model result.

2.2 System and observation models

We conduct an EnKF experiment by adding a system noise to the thermocline depth anomaly, which can be interpreted as an uncertainty in the prescribed monthly mean thermocline depth. We assume Gaussian system noise with zero mean and $(1 \text{ m})^2$ variance, equivalent to $(0.573 \text{ cm})^2$ variance for SSH. For the off-diagonal components of the covariance, horizontal correlations are given by a Gaussian type function with zonal and meridional length scales of L_x and L_y , respectively. Since the model thermocline depth anomaly is represented by the sum of the Kelvin and the Rossby components, we can choose any of those components to which system noise is added. In the present experiment, we add system noise to the Rossby component because it appears on the thermocline depth

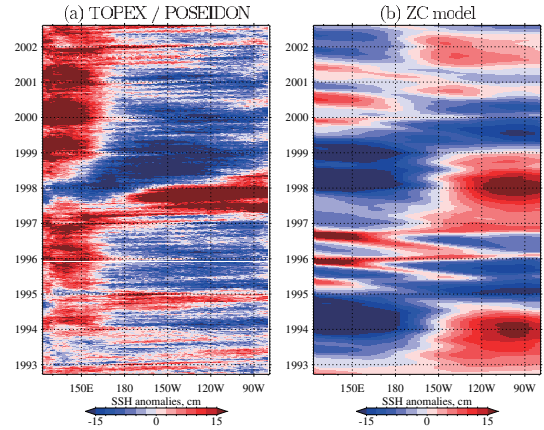


Fig. 1. Temporal variations of the SSH anomalies along the equator that are (a) observed by TOPEX/POSEIDON, and (b) reproduced by the ZC model.

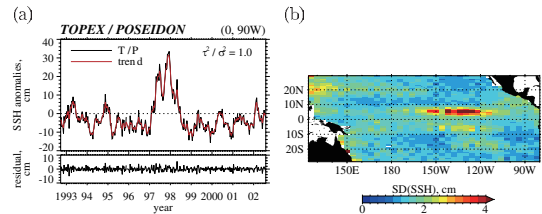


Fig. 2. (a) (Top) SSH anomaly observation (black) at equator and 90°W and its smoothed trend (red), and (Bottom) the residual between the observation and the smoothed value; (b) Diagonal elements of the observation noise covariance matrix (in the form of square root, standard deviation).

alone, while the Kelvin component also affects the zonal current anomaly (Cane and Patton 1984). Gaussian system noise realization is then slightly modified because it should be orthogonal to the Kelvin waves to keep the physical consistency. Specifically, we decompose the Gaussian noise into two components, orthogonal and non-orthogonal to the Kelvin wave, and use the former component as a system noise realization.

As mentioned in the previous subsection, the model SSH anomaly is linearly related to the thermocline depth anomaly. Thus the observation operator becomes a linear matrix. We then assume an observation matrix such that an observed SSH at each point is expressed by a weighted mean of the model thermocline depth anomalies with a correlation length of the model ocean grid size, $(2^\circ, 0.5^\circ)$.

We also assume a Gaussian for observation noise having zero mean. To construct the covariance matrix, we first treat the SSH anomaly data of each point as one dimensional time series and smooth it with the first-order trend model (Kitagawa and Gersch 1996). On the top panel of Fig. 2a shows the data and its smoothed trend at the equator and 90°W between September 23, 1992 to August 11, 2002 (T/P cycle 1 to 364), where the ratio of hyperparameters is fixed to 1. The bottom panel shows the residual between the original data and the smoothed value. Applying the same procedure to the other data points, we obtain residuals for all points inside the basin. With the residuals we calculate a sample covariance matrix and assume it to be the observation noise covariance matrix, whose diagonal elements are shown in Fig. 2b. While diagonal matrices have been often used for simplicity, the assumed observation noise covariance matrix has finite non-diagonal elements, which allow us to take account of the spatial correlation of the observation. In average, magnitude of the diagonal elements is $(1.48 \text{ cm})^2$, and zonal

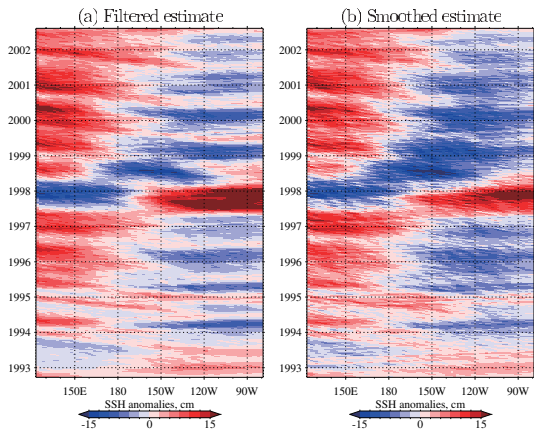


Fig. 3. Temporal variations of (a) the filtered and (b) the smoothed estimates of the SSH anomalies along the equator.

and meridional correlation scales are 2.38° and 2.52° , respectively. The magnitude is comparable to those used in the previous studies (Those of $(5 \text{ cm})^2$, $(1.7 \text{ cm})^2$, $(4 \text{ cm})^2$, and $(0.69 \text{ cm})^2$ were used in the adjoint, the representer, the ROKF, and the EKF studies, respectively. See Section 1.), and it is regarded as smaller than natural variations as shown in Figs. 1a and 2a.

2.3 EnKF and EnKS results

With 2,048 ensemble members, we run the EnKF procedure from T/P cycle 1 to cycle 364. Although there are variants of the EnKF (e.g., Evensen 2003, Section 2), what we use is the original form of the EnKF. We therefore apply neither multiplicative covariance inflation nor covariance localization. The number 2,048 is selected because it is larger than that of the maximum data points, 1,981; mathematically, the EnKF is not degraded when the ensemble size is greater than the number of independent observations (Ueno et al. 2006b).

The filtered SSH anomalies along the equator are shown in Fig. 3a. The filtered estimates appear to reproduce the observed variation after assimilation of the first six months: the 1997/98 ENSO event as well as the annual variations are identifiable in the filtered estimates. Figure 3b presents the smoothed estimates. Improvements can be found in the negative SSH anomalies reproduced in the central and eastern equatorial Pacific in 1999–2000, as well as in positive SSH anomalies in the western Pacific in the first 6 months.

The observation, the filtered estimate, and the smoothed estimate are compared in Fig. 4, which shows time evolution of the area-averaged SSH anomalies in the Niño 1 + 2, 3, 3.4, and 4 SST regions. Except for Niño 4, time delay in the filtered estimates was adjusted in the smoothed estimates. The retrieved negative anomalies found in Fig. 3b were clearly seen in Niño 3 and 3.4 in 1995 and during 1998–2000. The smoothed estimate in Niño 4 appeared to almost coincide with the filtered estimate.

While assimilated data are SSH anomalies alone, the coupled model can produce estimates of all of the variables included in the model. In Fig. 5 the smoothed estimates of the SST anomalies are compared with independent SST observations (Reynolds et al. 2002). We obtained the monthly anomalies by subtracting the mean values (from December, 1981 to February, 2006) from the original monthly data. Four panels are assigned to Niño 1 + 2, 3, 3.4 and 4 SST regions. The primary temporal characteristics of the smoothed estimate were similar to the observation, although the magnitude appeared slightly small.

Figure 6 shows temporal evolution of area-averaged wind anomalies for observation (NCEP Reanalysis 2 data) and the smoothed estimate. Plotted in Figs. 6a–c are three indices, which represent equatorial zonal wind anomalies in

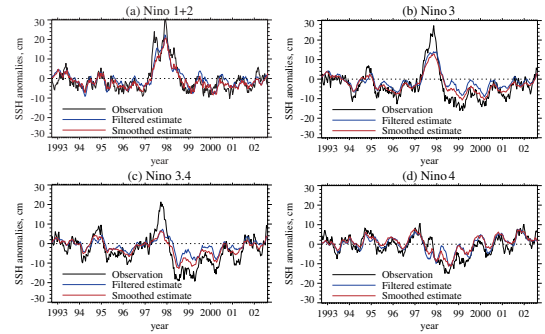


Fig. 4. Area-averaged SSH anomalies of the observation (black), the filtered estimate (blue), and the smoothed estimate (red) in (a) Niño 1 + 2 (0° – 10° S, 90° – 80° W), (b) Niño 3 (5° N– 5° S, 150° – 90° W), (c) Niño 3.4 (5° N– 5° S, 170° – 120° W), and (d) Niño 4 (5° N– 5° S, 160° E– 150° W).

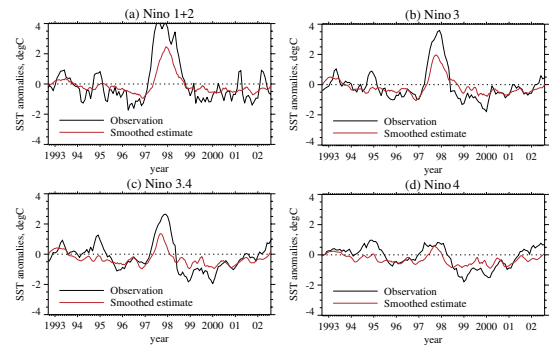


Fig. 5. Area-averaged SST anomalies of the observation (black) and of the smoothed estimate (red) in (a) Niño 1 + 2 (0° – 10° S, 90° – 80° W), (b) Niño 3 (5° N– 5° S, 150° – 90° W), (c) Niño 3.4 (5° N– 5° S, 170° – 120° W), and (d) Niño 4 (5° N– 5° S, 160° E– 150° W). Note that the smoothed estimate is obtained without SST data assimilation.

the western Pacific (5° N– 5° S, 135° E– 180°), the central Pacific (5° N– 5° S, 180° – 140° W), and the eastern Pacific (5° N– 5° S, 140° – 120° W). Those three regions are designated as TW1, TW2, and TW3, respectively. In TW1, the smoothed estimates reproduced easterly (negative) anomalies relatively well (in 1996, 1999, and 2000), while it gave poor estimates of westerly anomalies (in 1993, 1994, 1997, and 2002). Westerly anomalies in 1997 and 1998 are slightly retrieved in TW2, but the amplitude was still half of the observation. In TW3, the smoothed estimate appeared fairly better even for the westerlies and the reproduced temporal variations nearly coincided with that of the observation.

3. Summary and discussion

We have conducted EnKF and EnKS experiments that assimilate SSH anomaly observations to the intermediate coupled model. Although assimilated data were SSH anomalies alone, the obtained smoothed state can produce the estimates of all of the variables included in the model. Estimated SST anomalies around the equator were found to reproduce primary variations of the actual SSTs. In contrast, estimated wind anomalies had several aspects. For the zonal component, the smoothed estimate was consistent with the observation in the eastern Pacific regardless of its direction, that is, westerly or easterly. However, in the western Pacific, while easterly anomalies were properly reproduced, westerly anomalies did not appear in the smoothed estimate.

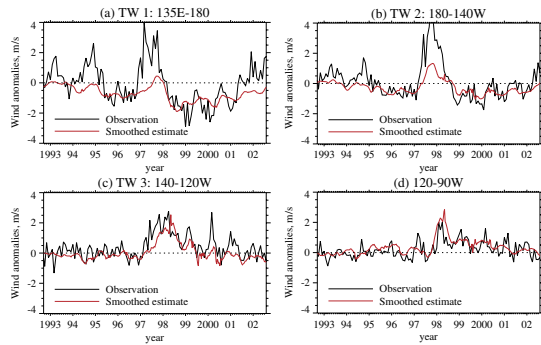


Fig. 6. Area-averaged zonal wind anomalies (positive westerly) for the observation (black) and for the smoothed estimate (red) in (a) TW1 (5°N – 5°S , 135°E – 180°), (b) TW2 (5°N – 5°S , 180° – 140°W), (c) TW3 (5°N – 5°S , 140° – 120°W), and (d) 5°N – 5°S , 120° – 90°W .

We now consider the cause of the lack of the westerlies in the western Pacific in the smoothed estimates. One reason may be the western limit (124°E) of the model ocean basin. Since the heating Q is assumed to be zero outside the rectangle ocean basin, the atmospheric wind u_a cannot be driven outside the boundary, and may be inadequate near the boundary. However, this does not appear to be the case. If it is, easterlies near the eastern boundary (80°W) should also be lacked in the smoothed estimate. On the other hand, easterlies are reproduced not only in the eastern Pacific of TW3 (140° – 120°W) but also in the further eastern region of 120° – 90°W as shown in Fig. 6d. The reproduced easterlies indicate that the lack of the westerlies is not simply due to the model western boundary.

Another cause may be that the approximated Kalman gain is smaller in the western Pacific than in the eastern Pacific. The smaller the gain is, the less the obtained smoothed state reflects the observation. System noise imposed on the Rossby component may also cause the lack of the westerly reproduction. In addition, we also expect that the westerly anomalies in the western Pacific is a missing physics by the ZC model. That is, the westerlies cannot be generated from the coupled interaction in the model, and, therefore, cannot be reproduced by the SSH anomaly assimilation due to the vanished covariance between the westerlies and the SSH.

The magnitude of the system noise, 1 m in thermocline depth anomaly, or equivalently 0.573 cm in SSH anomaly, may appear to be too small. Actually, an ensemble spread of the smoothed state often fails to capture observed short scale SSH variations (not shown). However, since the ZC model is an anomaly model, system noise imposed on anomaly variables should be small compared with the mean climatology. The adopted magnitude 1 m is set equal to the characteristics length scale of the thermocline depth anomaly of the ZC model, and too large system noise changes the model behavior in quality.

Acknowledgement

We would like to thank S. E. Zebiak for providing the code for the ZC model. The Altimeter Ocean Pathfinder TOPEX/POSEIDON SSH anomaly data were provided by the Physical Oceanography Distributed Active Archive Center (PO.DAAC) at the NASA Jet Propulsion Laboratory, Pasadena, California, from their Web site at <http://podaac.jpl.nasa.gov/>. NCEP Reanalysis 2 data were provided by the NOAA-CIRES Climate Diagnostics Center, Boulder, Colorado, USA, from their Web site at <http://www.cdc.noaa.gov/>. This research was partially supported by the Ministry of Education, Science, Sports and Culture, Grant-in-Aid for Young Scientists (B), 16700267, 2004–2007, and

by the Category 7 of MEXT RR2002 Project for Sustainable Coexistence of Humans, Nature and the Earth.

References

- Ballabrera-Poy, J., A. J. Busalacchi, and R. Murtugudde, 2001: Application of a reduced-order Kalman filter to initialize a coupled atmosphere-ocean model: Impact on the prediction of El Niño. *J. Climate*, **14**, 1720–1737.
- Bennett, A. F., B. S. Chua, D. E. Harrison, and M. J. McPhaden, 1998: Generalized inversion of Tropical Atmosphere-Ocean data and a coupled model of the tropical Pacific. *J. Climate*, **11**, 1768–1792.
- Bennett, A. F., B. S. Chua, D. E. Harrison, and M. J. McPhaden, 2000: Generalized inversion of Tropical Atmosphere-Ocean (TAO) data and a coupled model of the tropical Pacific. Part II: The 1995–96 La Niña and 1997–98 El Niño. *J. Climate*, **13**, 2770–2785.
- Cane, M. A., and R. J. Patton, 1984: A numerical model for low-frequency equatorial dynamics. *J. Phys. Oceanogr.*, **14**, 1853–1863.
- Chen, D., M. A. Cane, and S. E. Zebiak, 1999: The impact of NSCAT winds on predicting the 1997/1998 El Niño: A case study with the Lamont-Doherty Earth Observatory model. *J. Geophys. Res.*, **104**, 11321–11327.
- Chen, D., M. A. Cane, S. E. Zebiak, and A. Kaplan, 1998: The impact of sea level data assimilation on the Lamont model prediction of the 1997/98 El Niño. *Geophys. Res. Lett.*, **25**, 2837–2840.
- Chen, D., S. E. Zebiak, A. J. Busalacchi, and M. A. Cane, 1995: An improved procedure for El Niño forecasting: Implications for predictability. *Science*, **269**, 1699–1702.
- Evensen, G., 2003: The ensemble Kalman filter: theoretical formulation and practical implementation. *Ocean Dynamics*, **53**, 343–367.
- Fukumori, I., 2001: Data assimilation by models. *Satellite altimetry and earth sciences*, L.-L. Fu and A. Cazenave, eds., Academic Press, *International Geophysics Series*, **69**, 237–265.
- Kitagawa, G., and W. Gersch, 1996: *Smoothness priors analysis of time series*. Lecture Notes in Statistics, Springer-Verlag, New York, Inc., 261 pp.
- Latif, M., D. Anderson, T. Barnett, M. Cane, R. Kleeman, A. Leetmaa, J. O'Brien, A. Rosati, and E. Schneider, 1998: A review of the predictability and prediction of ENSO. *J. Geophys. Res.*, **103**, 14375–14393.
- Lee, T., J.-P. Boulanger, A. Foo, L.-L. Fu, and R. Giering, 2000: Data assimilation by an intermediate coupled ocean-atmosphere model: Application to the 1997–1998 El Niño. *J. Geophys. Res.*, **105**, 26063–26087.
- Miyoshi, T., 2005: Ensemble Kalman filtering – A meeting point between data assimilation and ensemble forecasting –. *Tenki*, **52**, 93–104 (in Japanese).
- Neelin, J. D., D. S. Battisti, A. C. Hirst, F. F. Jin, Y. Wakata, T. Yamagata, and S. E. Zebiak, 1998: ENSO theory. *J. Geophys. Res.*, **103**, 14261–14290.
- Reynolds, R. W., N. A. Rayner, T. M. Smith, D. C. Stokes, and W. Wang, 2002: An improved in situ and satellite SST analysis for climate. *J. Climate*, **15**, 1609–1625.
- Sun, C., Z. Hao, M. Ghil, and J. D. Neelin, 2002: Data assimilation for a coupled ocean-atmosphere model. Part I: Sequential state estimation. *Mon. Wea. Rev.*, **130**, 1073–1099.
- Ueno, G., T. Higuchi, T. Kagimoto, and N. Hirose, 2006a: Application of the ensemble Kalman filter to an atmosphere-ocean coupled model. *Nonlinear Statistical Signal Processing Workshop (NSSPW): Classical, Unscented and Particle Filtering Methods*, IEEE, Cambridge, UK.
- Ueno, G., T. Higuchi, T. Kagimoto, and N. Hirose, 2006b: Prediction of ocean state by data assimilation with the ensemble Kalman filter. *Joint 3rd International Conference on Soft Computing and Intelligent Systems and 7th International Symposium on advanced Intelligent Systems (SCIS & ISIS 2006)*, SOFT, Tokyo, Japan, 1884–1889.
- Zebiak, S. E., and M. A. Cane, 1987: A model El Niño–Southern Oscillation. *Mon. Wea. Rev.*, **115**, 2262–2278.